Natural killer cell infiltration is discriminative for antibody-mediated rejection and predicts outcome after kidney transplantation

Saleh Yazdani, Jasper Callemeyn, Stéphane Gazut, Evelyne Lerut, Henriette de Loor, Max Wevers, Line Heylen, Carole Saison, Alice Koenig, Olivier Thaunat, et al.

Natural killer cell infiltration is discriminative for antibody-mediated rejection and predicts outcome after kidney transplantation

OPEN

Saleh Yazdani[1,2,16], Jasper Callemeyn[1,2,16], Stéphane Gazut[3], Evelyne Lerut[4], Henriette de Loor[1], Max Wevers[1], Line Heylen[1,2], Carole Saison[5,6], Alice Koenig[5,6,7], Olivier Thaunat[5,6,7], Lieven Thorrez[8], Dirk Kuypers[1,2], Ben Sprangers[1,2], Laure-Hélène Noël[9], Leentje Van Lommel[10], Frans Schuit[10], Marie Essig[11], Wilfried Gwinner[12], Dany Anglicheau[9,13,14], Pierre Marquet[15] and Maarten Naesens[1,2]; for the BIOMARGIN Consortium

[1]*Laboratory of Nephrology, Department of Microbiology and Immunology, KU Leuven, Leuven, Belgium;* [2]*Department of Nephrology and Renal Transplantation, University Hospitals Leuven, Leuven, Belgium;* [3]*CEA, LIST, Laboratory for Data Analysis and Systems' Intelligence, Gif-sur-Yvette, France;* [4]*Department of Morphology and Molecular Pathology, University Hospitals Leuven, Leuven, Belgium;* [5]*U1111 INSERM, Lyon, France;* [6]*Department of Transplantation, Nephrology and Clinical Immunology, Edouard Herriot University Hospital, Lyon, France;* [7]*Claude Bernard University (Lyon-1), Lyon, France;* [8]*Department of Development and Regeneration, KU Leuven, Leuven, Belgium;* [9]*Necker-Enfants Malades Institute, French National Institute of Health and Medical Research U1151, Paris, France;* [10]*Gene Expression Unit, Department of Cellular and Molecular Medicine, KU Leuven, Leuven, Belgium;* [11]*CHU Limoges, Department of Nephrology, Dialysis and Transplantation, University of Limoges, Limoges, France;* [12]*Department of Nephrology, Hannover Medical School, Hannover, Germany;* [13]*Paris Descartes, Sorbonne Paris Cité University, Paris, France;* [14]*Department of Nephrology and Kidney Transplantation, RTRS Centaure, Necker Hospital, Assistance Publique-Hôpitaux de Paris, Paris, France; and* [15]*U850 INSERM, University of Limoges, CHU Limoges, Limoges, France*

Despite partial elucidation of the pathophysiology of antibody-mediated rejection (ABMR) after kidney transplantation, it remains largely unclear which of the involved immune cell types determine disease activity and outcome. We used microarray transcriptomic data from a case-control study (n = 95) to identify genes that are differentially expressed in ABMR. Given the co-occurrence of ABMR and T-cell–mediated rejection (TCMR), we built a bioinformatics pipeline to distinguish ABMR-specific mRNA markers. Differential expression of 503 unique genes was identified in ABMR, with significant enrichment of natural killer (NK) cell pathways. CIBERSORT (Cell type Identification By Estimating Relative Subsets Of known RNA Transcripts) deconvolution analysis was performed to elucidate the corresponding cell subtypes and showed increased NK cell infiltration in ABMR in comparison to TCMR and normal biopsies. Other leukocyte types (including monocytes/macrophages, CD4 and CD8 T cells, and dendritic cells) were increased in rejection, but could not discriminate ABMR from TCMR. Deconvolution-based estimation of NK cell infiltration was validated using computerized morphometry, and specifically associated with glomerulitis and peritubular capillaritis. In an external data set of kidney transplant biopsies, activated NK cell infiltration best predicted graft failure amongst all immune cell subtypes and even outperformed a histologic diagnosis of acute rejection. These data suggest that NK cells play a central role in the pathophysiology of ABMR and graft failure after kidney transplantation.

Kidney International (2019) **95,** 188–198; https://doi.org/10.1016/j.kint.2018.08.027

KEYWORDS: antibody-mediated rejection; gene expression; histology; kidney transplantation; natural killer cells; survival

The existing immunosuppressive armamentarium is insufficient in preventing kidney transplant recipients from developing humoral alloreactivity[1] with the occurrence of donor-specific antibodies (DSAs) to human leukocyte antigen (HLA) and ABMR, which is hallmarked by microcirculation inflammation and complement split product (C4d) deposition.[2,3] In recent years, DSAs were demonstrated to be a crucial prognostic factor for graft outcome and ABMR is recognized as a prime reason for graft failure after kidney transplantation.[4–6]

The underlying mechanisms of ABMR have been intensively studied over the past decade to identify potential therapeutic targets. Given the central role of anti-HLA antibodies in the occurrence of ABMR, B-cell inhibition (e.g., by B cell–depleting rituximab treatment), plasma cell inactivation (by proteasome inhibition using bortezomib), or HLA antibody depletion by plasma exchange or the IgG-degrading enzyme derived from *Streptococcus pyogenes* has been tested in clinical studies.[7] However, most of these therapies had only limited success in the prevention or treatment of ABMR.[8] Also, complement

Correspondence: *Maarten Naesens, Department of Nephrology and Renal Transplantation, University Hospitals Leuven, Herestraat 49, 3000 Leuven, Belgium. E-mail: maarten.naesens@uzleuven.be*

[16]Both authors contributed equally to this work.

Received 13 June 2018; revised 26 July 2018; accepted 16 August 2018; published online 3 November 2018

inhibition by eculizumab or other complement inhibitors is being tested in ABMR, but pilot data suggest that terminal complement inhibition is effective only in a subset of ABMR cases.[9–11] Therefore, novel and innovative preventive or therapeutic approaches for ABMR are needed to improve outcome after transplantation. Nevertheless, despite the partial elucidation of different processes that play a role in the pathophysiology of ABMR,[12] it remains largely unclear which of these pathways actually determine ABMR activity and outcome after transplantation and which processes are the most promising targets for the prevention and treatment of ABMR.

In this study we aimed to elucidate the pathways and the repertoire of graft-infiltrating immune cells that distinguish ABMR from TCMR and that determine graft outcome after kidney transplantation.

RESULTS

Patient population and phenotypes

Transcriptomic data from 95 samples of the Biomarkers of Renal Graft Injuries in Kidney Allograft Recipients (BIOMARGIN) case-control study, all pertaining to unique subjects, were used as the initial test cohort. ABMR was present in 15 of 95 cases (15.8%), TCMR in 11 of 95 cases (11.6%), and mixed rejection (ABMR + TCMR) in 6 of 95 cases (6.3%). The other 63 of 95 biopsies (66.3%) did not have rejection (no rejection). The demographic characteristics of this cohort are listed in Supplementary Tables S1 and S2. Patients with ABMR (including mixed cases) had significantly higher degrees of proteinuria (0.57 ± 0.64 g/l vs. 0.17 ± 0.42 g/l; $P = 0.001$) but similar estimated glomerular filtration rate (37.7 ± 18.2 ml/min per 1.73 m^2 vs. 43.6 ± 19.4 ml/min per 1.73 m^2; $P = 0.15$) than did patients without ABMR (TCMR or no rejection). C4d deposition was present in 45% of cases with ABMR.

Identification of ABMR-specific transcripts

Implementing the described statistical pipeline, 783 probe sets were found with a multivariate ABMR score of >0.25, reflecting discriminative performance for ABMR across all comparisons in the 95 samples of the BIOMARGIN study. The 783 selected probe sets represented ~1.5% of the transcripts. To further enrich the probe set list with ABMR-specific hits, 131 transcripts with a TCMR score of >0.20 were eliminated, which yielded 652 ABMR-specific transcripts, corresponding to 503 unique identified genes. In these 503 unique genes specific for ABMR, canonical pathway enrichment analysis of the identified transcripts using Ingenuity Pathway Analysis (Ingenuity Systems, Redwood City, CA) demonstrated significant enrichment of genes and pathways involved in innate and adaptive immunity, including graft versus host disease ($P < 0.001$), allograft rejection ($P < 0.001$), antigen presentation ($P < 0.001$), communication between the innate and adaptive immune systems ($P < 0.001$), crosstalk between dendritic and NK cells ($P < 0.001$), and NK cell signaling ($P < 0.001$) (Figure 1a; Supplementary Table S3).

Because these pathways share many genes, all genes from 6 of the top 10 pathways were selected and plotted in an overlapping (Figure 1b) and an interaction network (Figure 1c) structure. All genes except *TRGV9*, which was omitted from the interaction network, were strongly connected to each other, either directly or indirectly. Notably, interferon-gamma and tumor necrosis factor were at the center of this network, each regulating a large set of molecules associated with ABMR (140 and 143, respectively; more than one-third of all genes in the ABMR gene set: 196 of 503 genes). We then predicted upstream regulators within our ABMR gene set by using Ingenuity Pathway Analysis. Most of the top factors were cytokines such as interferon-gamma, tumor necrosis factor, and interleukins (Supplementary Table S4), which is also consistent with the central place of these cytokines in the network structure shown in Figure 1c. Transcription regulators were also predicted to explain differential expression of the ABMR gene set including *STAT1/3*, *IRF7*, *NKX2-3*, and *SMARCA4*. Interestingly, *STAT1*, *STAT4*, *IRF1*, and *IRF8* were also present in the ABMR gene set.

In Ingenuity Pathway Analysis of the 503 genes associated with ABMR (Supplementary Table S5), we noted significant enrichment of leukocyte activation (129 of 503 genes) and immune cell proliferation (131 of 503 genes). This observation was confirmed with Enrichr (a comprehensive gene set enrichment analysis web server) using public gene expression data from the human gene atlas,[13,14] which specifically showed enrichment of genes expressed in $CD56^+$ NK cells ($P < 0.001$), $CD14^+$ monocytes ($P < 0.001$), and $CD33^+$ myeloid cells ($P < 0.001$).

Deconvolution of immune cell distribution in ABMR

Considering that many of the differentially expressed transcripts were not specific for immune cell subsets, we next performed more detailed deconvolution analyses to elucidate the nature of the graft-infiltrating immune cell subsets. To estimate the differential relative leukocyte distribution among rejection types, the CIBERSORT algorithm[15] was applied to the transcriptomic data of the BIOMARGIN samples and an external validation cohort (GSE21374, a publicly available database). For this purpose, the LM22 gene signature matrix was used, which contains 547 genes that can distinguish between 22 leukocyte subtypes, corresponding to 11 major leukocyte types. In our cohort, a significantly higher relative percentage of NK cells in ABMR was demonstrated in comparison to TCMR and no rejection (Figure 2; Supplementary Figure S1A and Supplementary Table S6). Similarly, NK cell distribution was increased when considering mixed and "pure" ABMR cases, respectively.

To obtain an estimation of absolute leukocyte cell subset infiltration, we adjusted the CIBERSORT deconvolution data (relative fractions of 22 leukocyte subtypes) for the expression of the pan-leukocyte marker CD45/*PTPRC* (Supplementary Figure S2). We then correlated absolute leukocyte infiltration of all 11 major leukocyte types in the BIOMARGIN data set with different transplant rejection phenotypes (ABMR or TCMR) relative to infiltration in samples without rejection. Among the leukocyte types, NK cells, both resting and activated subtypes, were the only cells that differentiated ABMR from TCMR (Figure 3a and b; Supplementary Figure S1B). Other leukocyte types such as monocytes/macrophages, CD4

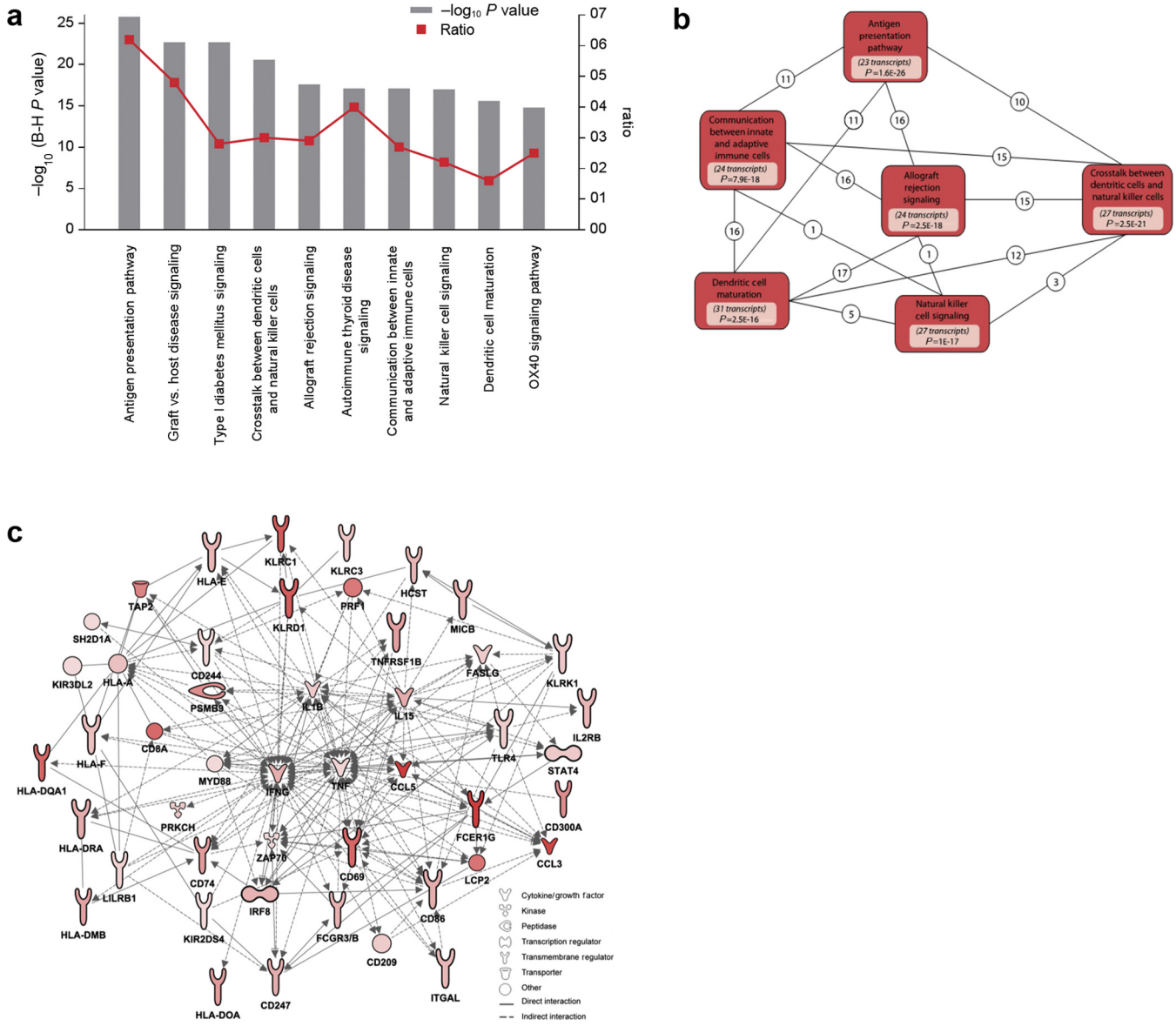

Figure 1 | Pathway enrichment analysis of antibody-mediated rejection (ABMR) transcripts. (**a**) The 652 ABMR identifiers (503 unique identified genes) were analyzed using Ingenuity Pathway Analysis. The figure shows the top 10 enriched canonical pathways with the Benjamini-Hochberg (B-H) multiple testing–corrected *P* values (calculated using the right-tailed Fisher exact test) as well as the number of genes in our set versus the total in each pathway (ratio). (**b**) This graph represents the number of significant genes (among the 503) that were shared between 6 of the top 10 enriched immune pathways. The number of genes used for each pathway, with the corresponding *P* value, is shown. The number of overlapping genes between each pathway is shown in the connecting lines. (**c**) The genes from these 6 immune pathways were plotted in a network structure. All of them (except *TRGV9*, which was omitted) were strongly connected to each other. Connections represent literature evidence of an interaction, either direct (physical binding, shown by solid lines) or indirect (e.g., influencing expression, shown by dashed lines). Red color intensity correlates with the observed fold change value of the individual gene.

and CD8 T cells, and dendritic cells were highly enriched in ABMR, but did not discriminate ABMR from TCMR (Supplementary Figure S2B).

NK cell infiltration and ABMR histology

Next, we studied whether NK cell infiltration is associated with the presence of DSAs and ABMR-specific histological lesions, such as microcirculation inflammation (defined as glomerulitis plus peritubular capillaritis) (Figure 3c). Of the 24 biopsies with microcirculation inflammation, 22 (91.7%) had NK cell infiltration above the median value (Figure 3d), with good discriminative performance (area under the receiver operating characteristic curve, 0.89; $P < 0.001$). There was no association between NK cell infiltration and transplant glomerulopathy. Tubulitis was also associated with estimated NK cell infiltration. All other lesions including interstitial inflammation and chronic histological lesions did not associate with NK cell infiltration. Of the 22 biopsies with both microcirculation inflammation score ≥2 and increased NK cell infiltration,

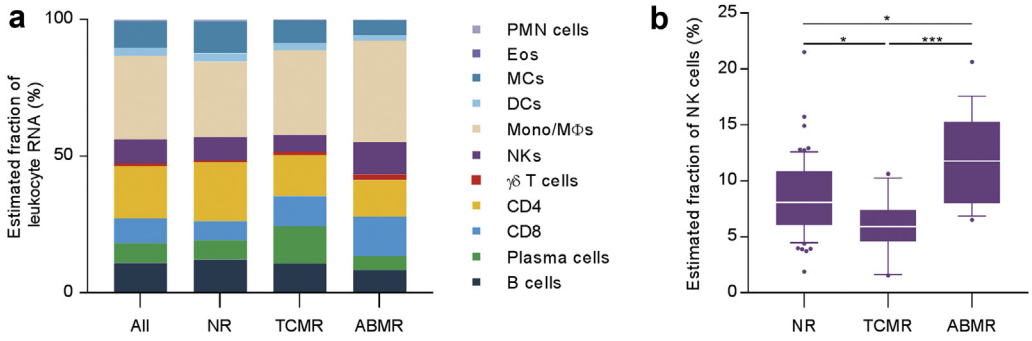

Figure 2 | Relative fraction of leukocytes and transplant rejection phenotype. (**a**) The CIBERSORT (Cell type Identification By Estimating Relative Subsets Of known RNA Transcripts) algorithm[15] was applied to the transcriptomic data of the BIOMARGIN samples. The averaged relative distribution of these 11 leukocyte types was compared by type of rejection (see also Supplemental Table S6). (**b**) A higher relative percentage of natural killer (NK) cells was demonstrated in antibody-mediated rejection (ABMR) than in T cell–mediated rejection (TCMR) and no rejection (NR) samples (box: interquartile range; line: median; whiskers: 10th and 90th percentile). *$P < 0.05$, **$P < 0.01$, ***$P < 0.001$. γδ T cell, gamma-delta T cell; CD4, CD4-positive T cell; CD8, CD8-positive T cell; DC, dendritic cell; Eo, eosinophil; HLA, human leukocyte antigen; MC, mast cell; Mono/MΦ, monocyte/macrophage; PMN, polymorphonuclear neutrophil.

15 (68.2%) had detectable DSAs. All 15 biopsies were classified as ABMR by central pathology. The remaining 7 cases (31.8%) did not have circulating DSAs, and 3 of these did not have any detectable HLA antibodies. The cause of the histology and molecular profile of these biopsies with microcirculation inflammation and molecular signs of NK cell infiltration, in the absence of DSAs, remained unknown. C4d deposition in peritubular capillaries was demonstrated in only 8 of 22 biopsies (36.3%) with a high estimated NK cell infiltration and microcirculation inflammation. All patients with C4d deposition in peritubular capillaries had increased NK cell infiltration (Figure 3e).

NKp46 immunohistochemistry and ABMR histology

To confirm the deconvolution-inferred NK cell increase in ABMR, computer-assisted histological quantification was used. We compared the density of NK cells between a subset of samples with ABMR (n = 9), samples with TCMR (n = 11), and samples without rejection (n = 9) by using the consensus phenotypic marker NKp46/CD335 (Figure 4a).[16] No mixed rejection phenotypes were included. ABMR samples had significantly higher NK cell infiltration than did samples without rejection (Figure 4b). The number of infiltrating NK cells significantly associated with the presence of DSAs, C4d deposition in peritubular capillaries, and microcirculation inflammation. Also, samples diagnosed with TCMR had higher NK cell infiltration than did samples without rejection. Although the NK cell count was higher in ABMR than in TCMR, this trend did not reach statistical significance. Nevertheless, individual lesions of TCMR such as tubulitis or interstitial inflammation did not associate with increased NK cell infiltration, illustrating that the molecular signatures of NK cell infiltration correspond better with the detailed and semiquantitative histological presentation than with the dichotomous histological diagnoses according to Banff consensus (Figure 4c).

Activated NK cells and graft failure

To evaluate which immune cell type associates with graft outcome, we applied the CIBERSORT algorithm with the LM22 gene signature matrix to a publicly available database (GSE21374),[16] comprising microarray data of 282 indication biopsies from 105 patients. Rejection was reported in 77 of 282 biopsies (27.3%), although no further information on the specific phenotype was available in the data set. Importantly, the occurrence of graft failure in the first 3 years postbiopsy was reported.

Similar to our study population, infiltration of all major leukocyte subtypes was increased in cases of rejection (Supplementary Table S6). However, activated NK cells were the leukocytes that best predicted graft failure at both 1 year and 2 years postbiopsy (area under the receiver operating characteristic curve, 0.74) (Figure 5a–c). Although intrarenal plasma cells were also predictive of graft failure, this association was lost when only biopsies with histologically proven rejection were considered but persisted for NK cells (data not shown). In multivariate Cox proportional hazards analysis, NK cell infiltration predicted graft failure better than ($P < 0.001$), and independent of, the diagnosis of rejection according to the Banff classification ($P = 0.039$).

DISCUSSION

In this study, we demonstrate that ABMR after kidney transplantation associates with an intrarenal expression signature enriched with immune-related pathways in general and NK cell pathways in particular. The specific association of NK cell infiltration with the diagnosis of ABMR and with microcirculation inflammation, estimated using immune cell deconvolution of microarray expression data, further corroborates the importance of NK cells in ABMR.

Although this is not the first article reporting the involvement of NK cells in ABMR, its importance lies in the demonstration that activated NK cells are the sole cell type

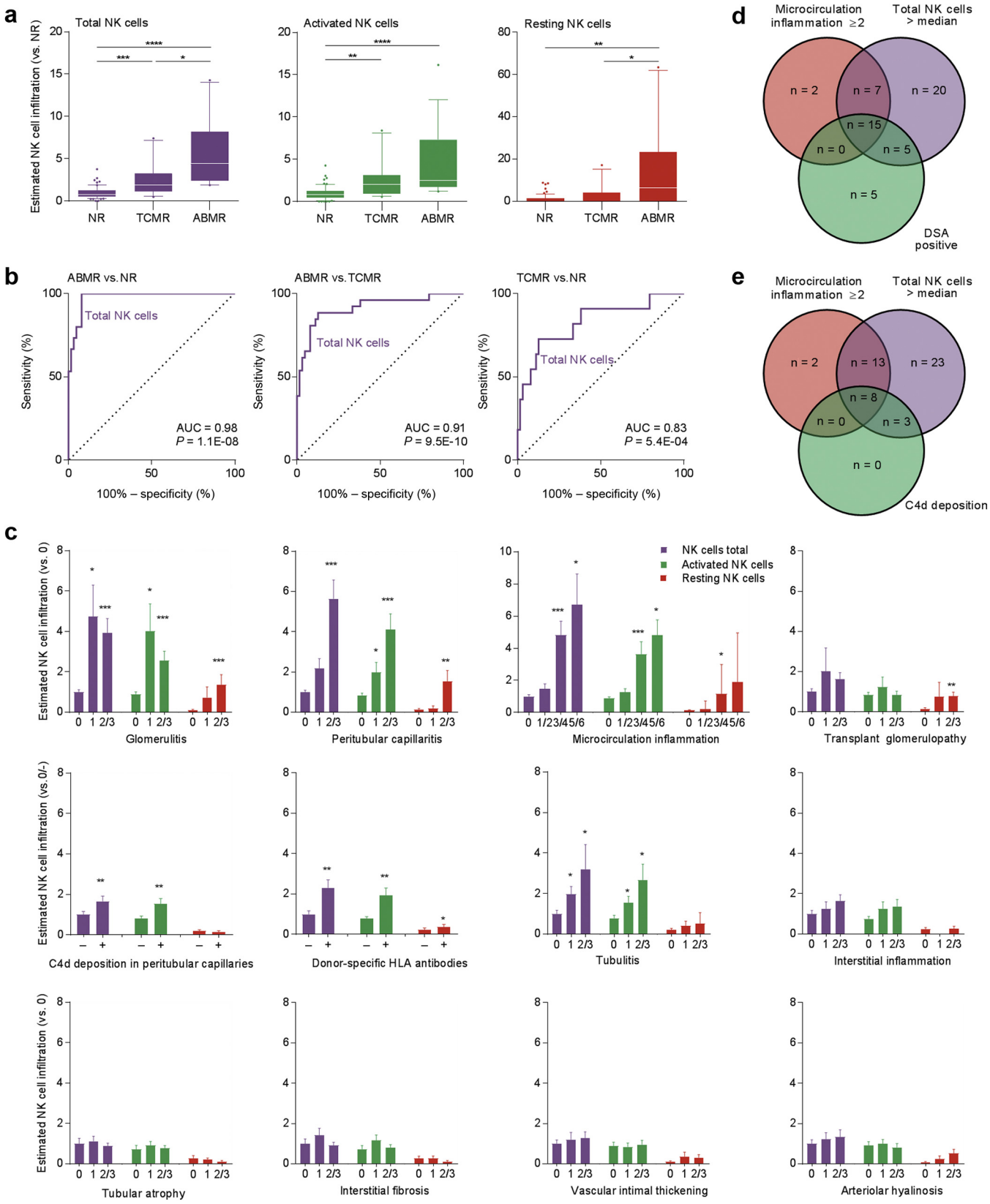

Figure 3 | Estimated absolute natural killer (NK) cell infiltration and its association with rejection phenotype and individual histological lesions. (**a**) Absolute NK cell infiltration was estimated by adjusting the relative percentage of total, activated, and resting NK cells from the CIBERSORT (Cell type Identification By Estimating Relative Subsets Of known RNA Transcripts) algorithm[15] for CD45 expression in the biopsy. Expression of activated and resting NK cells was higher in antibody-mediated rejection (ABMR) samples. (Continued)

that discriminates ABMR from TCMR and correlates with transplant outcome. We describe the specificity of NK cell infiltration for microcirculation inflammation, a hallmark of ABMR activity, whereas no association was found with other histological lesions such as interstitial inflammation and interstitial fibrosis. The lack of association with chronic lesions, including transplant glomerulopathy, may implicate a crucial role for NK cells in the early pathogenesis of active ABMR. An association of intrarenal NK cell transcripts with ABMR has been shown in a previous human study.[17] In contrast to our findings, this earlier study showed that a DSA-associated signature could not differentiate ABMR from TCMR while NK cell–selective transcripts associated with the presence of DSAs and microcirculation inflammation in late, but not in early, ABMR biopsies. This leads to questions about the specificity of these transcripts for ABMR.[18]

The more specific NK cell signatures for ABMR in our BIOMARGIN set are likely explained by the case-control study design and focus on well-defined single pathologist histological phenotyping, including only few mixed cases, whereas the previous analyses had a cross-sectional study design and less centralized phenotyping methods. In addition, in our study, the proportions of ABMR cases and TCMR cases occurring within the first transplant year compared with those occurring at later time points were similar, which probably minimized the influence of time-dependent lesions and transcripts that was seen in these previous studies.[19]

A similar NK cell profile was recently reported in heart transplantation, where NK cell, endothelial cell/angiogenesis, monocyte, and interferon-gamma–inducible transcripts were the main molecular signatures of cardiac ABMR.[20] This corroborates the general validity of our findings and the potential canonical value of these ABMR signatures across different organ types. The importance of NK cells in ABMR in humans is supported by animal studies that provided compelling evidence that these cells are involved in cardiac and kidney ABMR.[17,18,21–26]

Mechanistically, although a strong association with NK cell infiltration is demonstrated, it is unclear where they are involved in the pathogenesis of ABMR, that is, as a late downstream effector or as an early mediator directly triggered by DSAs. After transplantation, NK cells were shown to be primarily involved in complement-independent rejection mechanisms, such as antibody-dependent cellular cytotoxicity (ADCC), in both animal models and human studies.[21,27] Indeed, whole-genome and targeted expression analyses also suggested that ADCC plays a role in acute ABMR.[28–30] It has also been shown that increased ADCC reactivity can be used to predict the development of chronic allograft injury in kidney transplant recipients, even independent of DSA detection.[31] Lately, Parkes *et al.*[32] studied CD16a-inducible transcripts in primary human NK cells *in vitro* and showed the involvement of some of these transcripts in NK cell activation in ABMR, including the central involvement of interferon-gamma, tumor necrosis factor, and colony-stimulating factor 2, which we also identified as key upstream regulators in our ABMR signature.

The importance of NK cells in ABMR seems contradictory to the observed small relative fraction, as they constitute only a minority of infiltrating leukocytes. In addition, NK cells have an important role in producing cytokines and chemokines and interact with other immune and nonimmune cells. The action of very few infiltrating cells could thus be much broader than is perhaps suggested by their numbers. Although this might implicate a rather immunoregulatory role for NK cells, another explanation may be offered by considering the effector site. DSAs interact with the vascular endothelium and trigger multiple effector mechanisms, including ADCC, which are initiated in the dynamic endovascular compartment. Blood circulation may allow rapid clearance of a majority of NK cells, with only a minority infiltrating into the perivascular compartment. Further characterization of the infiltrating NK cell is necessary to investigate their origin (tissue-resident vs. infiltrating peripheral blood cell), reactivity (expression of CD16, killer-cell immunoglobulin-like receptor, etc.), and effector mechanism (regulatory vs. cytotoxic).

Of all the cases with NK cell infiltration and microvascular inflammation, 62% did not have C4d deposition in peritubular capillaries, whereas all cases with C4d deposition had increased NK cell presence. Although C4d deposition can be a useful epiphenomenon for the diagnosis of ABMR, this suggests that complement activation and C4d deposition are not necessary for NK cell–mediated graft injury, which is supported by the variable results of studies on complement inhibitors for this disease.[9–11]

Despite the association between NK cell infiltration, ADCC, and ABMR in one-third of cases with microvascular inflammation and increased NK cell infiltration, no circulating DSAs were detected. This finding remains ill-explained and could be related to intragraft adsorption of DSAs or presence of non-HLA DSAs, which therefore remain

Figure 3 | (Continued) (**b**) Logistic regression analysis illustrated the association between ABMR and estimated total NK cell infiltration according to CIBERSORT. (**c**) Based on the observed associations of estimated NK cell infiltration with ABMR, the relation of Banff-graded individual histological lesions and the presence/absence of donor-specific antibodies (DSAs) with CIBERSORT-estimated NK cell infiltration was evaluated. Both total and activated NK cells showed a significant association with ABMR-defining histological lesions such as glomerulitis, peritubular capillaritis, and microcirculation inflammation. In contrast, other histological lesions such as interstitial inflammation, tubular atrophy, transplant glomerulopathy, and interstitial fibrosis did not show any association with estimated NK cell infiltration. The number of cases with intimal arteritis (Banff "v" lesions) was too low (n = 3) and is not represented separately in this graph. (**d,e**) In these Venn diagrams, the number of biopsies with DSAs, microcirculation inflammation, complement (C4d) deposition, and increased total NK cell infiltration (defined as above median values) are depicted. Numbers do not match because of lack of C4d staining or information on DSA status in 2 cases, respectively. AUC, area under the curve; NR, no rejection; TCMR, T cell–mediated rejection.

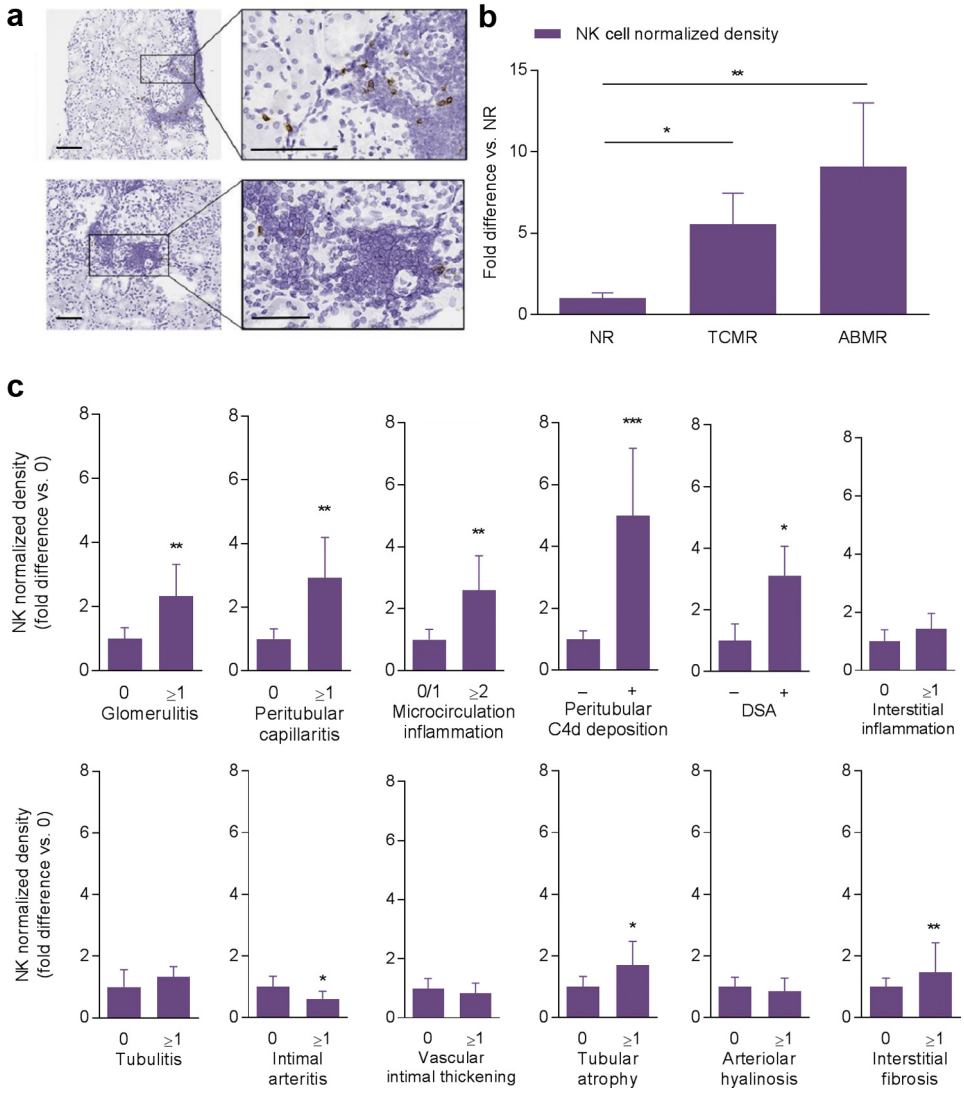

Figure 4| Counted natural killer (NK) cell infiltration and its association with rejection phenotype and individual histological lesions. **(a)** NK cell infiltration was determined after immunohistochemical staining in a subset of samples with antibody-mediated rejection (ABMR; n = 9), T cell–mediated rejection (TCMR; n = 11), and no rejection (NR; n = 9). From top to bottom: Representative examples of kidney graft biopsies with, respectively, rich and poor NK cell infiltration. Bar = 100 μm. **(b)** Normalized density of NK cells in normal biopsies was used as reference. This graph showed a significant NK cell fold increase for ABMR versus NR samples, but also for TCMR versus NR samples, albeit to a lesser extent. The NK cell normalized density was measured using computerized histomorphological analysis. **(c)** The relation of Banff-graded individual histological lesions and the presence/absence of donor-specific antibodies (DSAs) with measured NK cell infiltration was evaluated. As depicted here, NK cell infiltration showed a significant fold increase in ABMR-defining histological lesions such as peritubular capillaritis, glomerulitis, microvascular inflammation, and complement (C4d) deposition in peritubular capillaries in comparison to those without a lesion. In contrast, other histological lesions, associated with TCMR, such as interstitial inflammation and tubulitis showed no significant associations with NK cell infiltration. A significant fold increase in NK cell infiltration is shown in samples with the presence of DSAs versus absence of DSAs. $^{*}P < 0.05$, $^{**}P < 0.01$, $^{***}P < 0.001$ compared to 0 score. To optimize viewing of this image, please see the online version of this article at www.kidney-international.org.

undetected.[33] However, antibody-independent NK cell activation, for example, through endothelial stress ligands or missing self, should be considered.[20,23,24,34,35] Given the evidence on the importance of NK cells in transplant injury in preclinical models, independent of antibody presence, and the suggestion of this phenomenon in our clinical study, more work needs to be done to elucidate the prevalence and importance of antibody-independent factors in NK cell–mediated injury to kidney allografts.

Identification of the underlying NK cell stimulus in the renal allograft infiltration appears challenging. Currently available clinicopathological parameters provide only indirect etiological clues. Elucidation of NK cell subtypes within the allograft may identify populations that are more prone to a specific stimulus (e.g., $CD56^{dim}$ cells express CD16 and can elicit ADCC).[36] Flow cytometry of renal allograft tissue has recently been described[37] and may offer more detail about the characteristics of infiltrating NK cells. However, because most

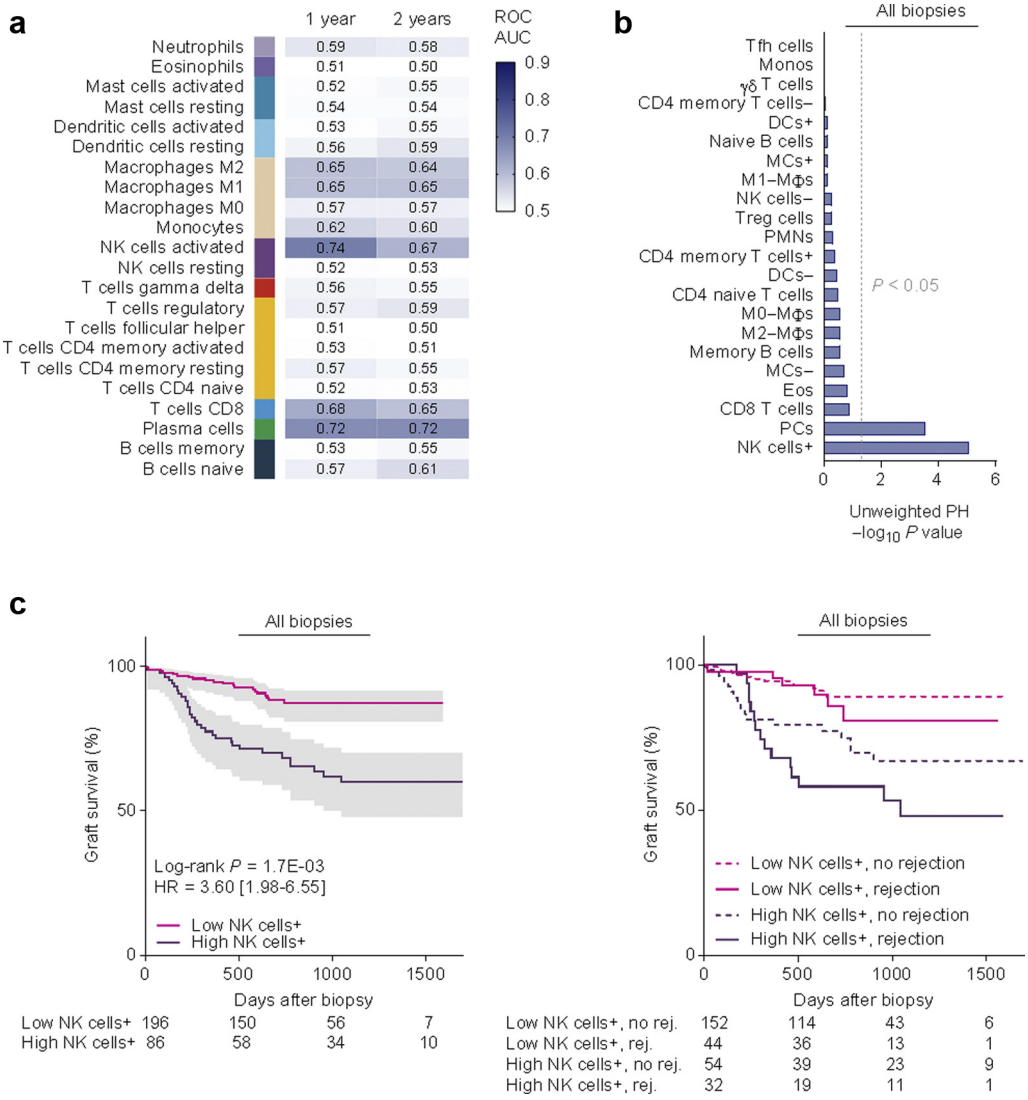

Figure 5 | Activated natural killer (NK) cell transcripts associate with graft failure. To identify which immune cell types associated with graft failure, logistic regression analysis (area under the receiver operating characteristic curve [ROC AUC]) of the CIBERSORT (Cell type Identification By Estimating Relative Subsets Of known RNA Transcripts)–derived relative leukocyte estimation was performed on the GSE21374 data set for graft failure at 1 and 2 years posttransplant. (**a**) Heat map of ROC AUC data shows that among all 22 different cell types, activated NK cells have the highest discriminative power in predicting graft failure at both 1 year and 2 years postbiopsy when considering all biopsies (AUC, 0.74). (**b**) Cox proportional hazard (PH) analyses confirm that among all leukocytes, activated NK cell infiltration predicted graft failure most significantly. (**c**) Kaplan-Meier survival curves illustrate the high hazard ratios for graft failure from the estimation of activated NK cell infiltration according to the mean of NK cell infiltration across the data set (left panel). In multivariate Cox proportional hazards analysis, NK cell infiltration predicted graft failure better ($P < 0.001$) than, and independent of, the diagnosis of rejection according to the Banff classification ($P = 0.039$) (right panel). γδ T cell, gamma-delta T cell; CI, confidence interval; DC, dendritic cell; Eo, eosinophil; HR, hazard ratio; MΦ, macrophage; MC, mast cell; Mono, monocyte; PMN, polymorphonuclear neutrophil; T fh cell, follicular helper T cells; Treg cell, regulatory T cells.

ligand-receptor interactions are not sufficient as a single stimulus, caution should be exercised when inferring etiology on the basis of the phenotype of this innate immune cell. Finally, from a mechanistic viewpoint, ADCC and other cytotoxic pathways do not appear mutually exclusive and may perhaps elicit a synergistic effect in the renal allograft.

In an external cohort, among all immune cell subtypes, we also showed that infiltration of activated NK cells best predicted graft failure, even better than histology of acute rejection. One could argue that the prognostic significance of intragraft NK cell infiltration merely reflects the negative outcome that is associated with rejection in general, because NK cells are also upregulated in TCMR. However, a similar effect would then be expected for other immunological cell types but was demonstrated only to a lesser extent for plasma cells. NK cells, but not plasma cells, uniquely predicted graft failure in biopsy-proven rejection, supporting our findings that NK cell infiltration is a differentiating trait in renal allograft rejection. We hypothesize this association to be attributable to the inferior survival in ABMR in the current immunosuppressive era. Interestingly, estimating NK cell infiltration using CIBERSORT outperformed histological

rejection as a prognostic tool for graft failure. The latest revisions of the Banff classification have acknowledged the limited sensitivity of microscopy and encourage the use of molecular markers as alternative diagnostic criteria for ABMR. To our knowledge, estimation of immune cell infiltration through deconvolution analysis of transcriptomic data, although well established in tumor immunobiology, has not been used previously for this purpose. Although further validation in independent cohorts is obviously needed, the robust signal of NK cells, both in a case-control and in a longitudinal setting, appears promising.

Our study has several limitations. First, this study describes relatively few ABMR cases, including mixed phenotypes. To address this issue, the described statistical pipeline was specifically built to disentangle potentially mixed genetic signals in said samples when calculating an ABMR and TCMR score. However, in the deconvolution analysis, pure and mixed ABMR cases were grouped together. This may explain the association that was initially found between NK cells and tubulitis but that disappeared when immunohistochemical NK cell staining was performed on pathology slides of "pure" ABMR cases. Nonetheless, also in mixed ABMR cases, NK cell infiltration was significantly increased in comparison to TCMR. Second, the accuracy of the CIBERSORT algorithm in describing intrarenal immune cell populations has not been studied to our knowledge. We partially validated this approach by immunohistochemical confirmation of predicted NK cell infiltration in association with specific histological lesions, which suggests the robustness of this model in renal tissue. Finally, in the GSE21374 database, no information on the specific rejection phenotype was available, therefore impeding assessment of the diagnostic accuracy for ABMR. Moreover, the 2009 Banff criteria for TCMR and ABMR were used in this cohort as a definition for rejection, and have been significantly refined since then, which may in part explain the superior performance of the molecular NK cell marker.

In conclusion, our data indicate the potential of NK cell activation transcripts as pathogenesis-linked markers for the diagnosis and prognosis of ABMR in kidney transplantation. Further investigations are warranted to evaluate the diagnostic and prognostic performance of specific NK cell activation markers in the real-life setting. NK cell activation might be a valuable target for the development of novel therapies to improve outcome after kidney transplantation.

METHODS

Patients and sample collection

In the observational 3xBIOS^2 case-control substudy of the BIOMARGIN project (www.biomargin.eu; ClinicalTrials.gov identifier NCT02832661), samples from kidney transplant recipients were prospectively collected in 4 European clinical transplant centers: (i) University Hospitals Leuven, Belgium; (ii) Hôpital Necker Paris, France; (iii) Medizinische Hochschule Hannover, Germany; and (iv) Centre Hospitalier Universitaire Limoges, France. At each European clinical transplant center, the institutional review board and national regulatory agency approved the study and all participants provided written informed consent before inclusion in the study. All clinical, histological, and sample data were collected in a centralized electronic case report form, maintained by a clinical coordinating center. Only single kidney allograft recipients at least 18 years of age were included. Samples for this study were collected between October 2, 2012, and December 27, 2013, and case selection (N = 121) was performed in April 2014 on the basis of clinical and histological presentation. Biopsies were performed at the time of graft dysfunction or at protocol-specified moments, independent of graft function, according to local center practice. All biopsies included in this study were sent to the central pathology core of the 3xBIOS^2 substudy and rescored semiquantitatively according to the updated Banff classification, which implies that all biopsies were assessed using the same diagnostic criteria, regardless of the transplant center or the collection date.[38,39] No previously described molecular markers were assessed for the diagnosis of ABMR. In addition, we used microarray gene expression data from an external cohort that were described by Einecke *et al.*[40] (GSE21374) and made publicly available in the Gene Expression Omnibus of the National Institutes of Health (http://www.ncbi.nlm.nih.gov/geo/).[19,40,41]

Biopsy sample collection and preparation

Biopsy samples were collected according to a standardized sample collection procedure common to the 4 clinical transplant centers. Of each renal allograft biopsy included in this study, at least one-half of a core was immediately stored in Allprotect Tissue Reagent (QIAGEN Benelux B.V., Venlo, The Netherlands) and, after incubation at 4°C for at least 24 hours and maximum 72 hours, stored locally at −20°C until shipment to the Laboratory of Nephrology of the KU Leuven. We performed RNA extraction using the Allprep DNA/RNA/miRNA Universal Kit (QIAGEN Benelux B.V.) in a QIAcube instrument (QIAGEN Benelux B.V.). The quantity (absorbance at 260 nm) and purity (ratio of the absorbance at 230, 260, and 280 nm) of RNA isolated from biopsies were measured using the NanoDrop ND-1000 spectrophotometer (Thermo Scientific, Life Technologies Europe B.V., Ghent, Belgium). RNA integrity was evaluated using the Eukaryote Nano/Pico RNA Kit (Agilent Technologies Belgium NV, Diegem, Belgium) in the 2100 Bioanalyzer instrument (Agilent Technologies Belgium NV). Samples were stored at −80°C until further analysis.

Microarray gene expression analysis

RNA extracted from the BIOMARGIN biopsy samples was first amplified and biotinylated to complementary RNA using the GeneChip 3′ IVT PLUS Reagent Kit (Affymetrix Inc., High Wycombe, UK) and subsequently hybridized onto the GeneChip Human Genome U133 Plus 2.0 Array (Affymetrix Inc.), which covers >54,000 transcripts, according to the manufacturer's instructions. Arrays were scanned using the GeneChip Scanner 3000 7G System (Affymetrix Inc.), and image files were generated using the GeneChip Command Console Software. Finally, Robust Multichip Average background correction and normalization were performed using the Affymetrix Expression Console Software and expression values were log2 scaled. Of the 121 biopsies that were sent to the Laboratory of Nephrology, 109 survived prehybridization quality control checks and were analyzed. Outlier analysis and filtering were performed using the Hotelling's *T*-squared test on principal component analysis components and

quantile distribution of the profiles, which left 95 biopsies for further statistical analysis.

NK cell quantification using computerized histomorphological analysis

Immunostaining was performed on kidney biopsies from KU Leuven that were included in the BIOMARGIN study by using the consensus phenotypic marker NKp46/CD335,[16] which is highly conserved in mammals. Eight-micrometer kidney biopsy sections were stored at −80°C after being fixed in acetone. Before staining, kidney biopsies were thawed and rehydrated 5 minutes in phosphate-buffered saline. Staining was performed with EnVision G|2 Doublestain System, Rabbit/Mouse (DAB+/Permanent Red) kit (code K5361, DAKO, Les Ulis, France) according to the manufacturer instructions. Briefly, after neutralization of the endogenous peroxidases and saturation, each slide was stained with mouse anti-human NKp46 clone 9E2 (BioLegend) or isotype control (clone MOPC21, BioLegend, Koblenz, Germany) at a 1:100 dilution in phosphate-buffered saline for 1 hour. To reveal NKp46-positive cells, polymer/horseradish peroxidase (incubation time, 30 minutes) and chromogen 3,3'-diaminobenzidine (incubation time, 5 minutes) were used. Nuclei were counterstained with hematoxylin. Then, slides were dried and mounted on Diamount (Diapath, Martinengo, Italy). For computerized-assisted quantification of NK cell infiltration, slides were scanned and images were analyzed using a custom-made macro in Aperio ImageScope (Leica Biosystems, Nanterre, France) and FIJI software.[42] The density, that is, the number of NKp46-positive cells normalized to the surface of biopsy analyzed, was calculated in a minimum of 2 sections for each sample.

Statistical analysis

For variance analysis of continuous variables in different groups, nonparametric Wilcoxon-Mann-Whitney *U* test, nonparametric analysis of variance, and parametric 1-way analysis of variance were used. Data are presented as mean ± SEM. Dichotomous variables were compared using the chi-square test. Robust Multichip Average–normalized mRNA expression data of the biopsy samples were analyzed in a statistical pipeline developed using the R framework and designed for the purpose of the 3xBIOS[2] substudy. The statistical pipeline was an extension of the biosigner R package through which a predictive score was calculated. A multivariate score of >0.25 was considered as specific for ABMR and/or TCMR. For the purpose of this study, we added elastic net and shrunken centroids multivariate methods to sparse partial least squares regression, random forest regression, and support vector machine recursive feature elimination multivariate methods already available in the biosigner package.[43] Differentially expressed genes were analyzed using Ingenuity Pathway Analysis to assess their biological functions and upstream regulators. Pathway enrichment was calculated using the right-tailed Fisher exact test with Benjamini-Hochberg multiple testing–corrected *P* values. In addition, enrichment analysis was confirmed using Enrichr to compare genes in the differential set with public gene expression data of different cell types present in the human gene atlas.[13,14] Next, a computational machine learning method called CIBERSORT was used for deconvolution analysis of the heterogeneity of biopsies.[15] This algorithm enables analysis of the heterogeneity of infiltrating immune cells in complex solid tissues, primarily malignant tumors, by calculating the relative fraction of different phenotypes of human hematopoietic cells (11 major leukocyte types and 22 leukocyte subtypes of shared lineage, called *leukocyte signature matrix*, LM22) in tissue samples on the basis of the expression of 547 genes. Specifically for NK cells, gene signatures for resting and activated subtypes were derived from a study by Abbas *et al.*, who identified specific probe sets through deconvolution of microarray expression data.[44] In the deconvolution analysis, ABMR and mixed phenotypes (i.e., concurrent ABMR and TCMR) were considered as one group. The CIBERSORT algorithm was applied to the external data set described above. We used SAS 9.3 (SAS Institute, Cary, NC) for statistical analysis and GraphPad Prism 7 (GraphPad Software, San Diego, CA) for data presentation.

DISCLOSURE

All the authors declared no competing interests.

ACKNOWLEDGMENTS

We thank the clinical centers of the BIOMARGIN consortium, the clinicians and surgeons, nursing staff, and the patients. We also thank the contributions of Philippe Rinaudo and Etienne Thévenot to the initial data analysis. We thank Aline Schindelé and the team at Venn Life Sciences (France) for their invaluable help with sample collection, annotation, shipment, and the electronic case report form database. We acknowledge Philip Halloran and Luis Hidalgo for access to their public data and for their valuable suggestions on this article. The BIOMARGIN study is funded by the Seventh Framework Programme (FP7) of the European Commission, in the HEALTH.2012.1.4-1 theme of "innovative approaches to solid organ transplantation" (grant agreement no. 305499). MN was also funded by a C3 internal grant from the KU Leuven (grant no. C32/17/049).

AUTHOR CONTRIBUTIONS

MN, DA, WG, ME, and PM designed the study. MN, SY, JC, SG, LH, MW, OT, and LT performed data analysis and interpretation. MN, DA, WG, ME, HdL, BS, DK, LVL, and FS were involved in sample collection, sample extraction, and quality control as well as in microarray experiments. OT, CS, and AK performed NKp46 staining and computerized histomorphological assessments. EL and LHN performed histological analyses. MN, SY, and JC wrote the manuscript, and all coauthors revised it.

DATA AND MATERIALS AVAILABILITY

BIOMARGIN CEL files and normalized signal intensities are available in the Gene Expression Omnibus of the National Institutes of Health (http://www.ncbi.nlm.nih.gov/geo).

SUPPLEMENTAL MATERIAL

Figure S1. Estimated leukocyte infiltration and association with transplant rejection phenotypes in the BIOMARGIN study.
Figure S2. Relative expression of CD45/PTPRC according to the rejection phenotype.
Table S1. Demographic data of the 95 patients from the BIOMARGIN study.
Table S2. Histological data of the 95 biopsies from the BIOMARGIN study.
Table S3. Top 10 enriched canonical pathways in the 652 ABMR-specific transcripts. These 652 probesets correspond to 503 unique identified genes. Enrichment was calculated using IPA.
Table S4. Top 30 IPA upstream regulators in the 503 ABMR gene set.
Table S5. Top 30 gene functions of the 503 ABMR gene set according to Ingenuity Pathway Analysis.
Table S6. Relative fraction of the 11 leukocyte types in BIOMARGIN and GSE21374 data sets according to the biopsy phenotype.

Supplementary material is linked to the online version of the paper at www.kidney-international.org.

REFERENCES

1. Thaunat O, Koenig A, Leibler C, et al. Effect of immunosuppressive drugs on humoral allosensitization after kidney transplant. *J Am Soc Nephrol*. 2016;27:1890–1900.
2. Nankivell BJ, Alexander SI. Rejection of the kidney allograft. *N Engl J Med*. 2010;363:1451–1462.
3. Loupy A, Hill GS, Jordan SC. The impact of donor-specific anti-HLA antibodies on late kidney allograft failure. *Nat Rev Nephrol*. 2012;8:348–357.
4. El-Zoghby ZM, Stegall MD, Lager DJ, et al. Identifying specific causes of kidney allograft loss. *Am J Transplant*. 2009;9:527–535.
5. Sellares J, de Freitas DG, Mengel M, et al. Understanding the causes of kidney transplant failure: the dominant role of antibody-mediated rejection and nonadherence. *Am J Transplant*. 2012;12:388–399.
6. Naesens M, Kuypers DR, De Vusser K, et al. The histology of kidney transplant failure: a long-term follow-up study. *Transplantation*. 2014;98:427–435.
7. Jordan SC, Lorant T, Choi J, et al. IgG endopeptidase in highly sensitized patients undergoing transplantation. *N Engl J Med*. 2017;377:442–453.
8. Sandal S, Zand MS. Rational clinical trial design for antibody mediated renal allograft injury. *Front Biosci (Landmark Ed)*. 2015;20:743–762.
9. Jordan SC, Choi J, Kahwaji J, et al. Complement inhibition for prevention and treatment of antibody-mediated rejection in renal allograft recipients. *Transplant Proc*. 2016;48:806–808.
10. Kulkarni S, Kirkiles-Smith NC, Deng YH, et al. Eculizumab therapy for chronic antibody-mediated injury in kidney transplant recipients: a pilot randomized controlled trial. *Am J Transplant*. 2017;17:682–691.
11. Lefaucheur C, Viglietti D, Hidalgo LG, et al. Complement-activating anti-HLA antibodies in kidney transplantation: allograft gene expression profiling and response to treatment. *J Am Soc Nephrol*. 2018;29:620–635.
12. Halloran PF, Reeve JP, Pereira AB, et al. Antibody-mediated rejection, T cell-mediated rejection, and the injury-repair response: new insights from the Genome Canada studies of kidney transplant biopsies. *Kidney Int*. 2014;85:258–264.
13. Chen EY, Tan CM, Kou Y, et al. Enrichr: interactive and collaborative HTML5 gene list enrichment analysis tool. *BMC Bioinformatics*. 2013;14:128.
14. Kuleshov MV, Jones MR, Rouillard AD, et al. Enrichr: a comprehensive gene set enrichment analysis web server 2016 update. *Nucleic Acids Res*. 2016;44:W90–W97.
15. Newman AM, Liu CL, Green MR, et al. Robust enumeration of cell subsets from tissue expression profiles. *Nat Methods*. 2015;12:453–457.
16. Walzer T, Blery M, Chaix J, et al. Identification, activation, and selective in vivo ablation of mouse NK cells via NKp46. *Proc Natl Acad Sci U S A*. 2007;104:3384–3389.
17. Hidalgo LG, Sis B, Sellares J, et al. NK cell transcripts and NK cells in kidney biopsies from patients with donor-specific antibodies: evidence for NK cell involvement in antibody-mediated rejection. *Am J Transplant*. 2010;10:1812–1822.
18. Hidalgo LG, Sellares J, Sis B, et al. Interpreting NK cell transcripts versus T cell transcripts in renal transplant biopsies. *Am J Transplant*. 2012;12:1180–1191.
19. Halloran PF, Pereira AB, Chang J, et al. Microarray diagnosis of antibody-mediated rejection in kidney transplant biopsies: an international prospective study (INTERCOM). *Am J Transplant*. 2013;13:2865–2874.
20. Loupy A, Duong Van Huyen JP, Hidalgo L, et al. Gene expression profiling for the identification and classification of antibody-mediated heart rejection. *Circulation*. 2017;135:917–935.
21. Hirohashi T, Chase CM, Della Pelle P, et al. A novel pathway of chronic allograft rejection mediated by NK cells and alloantibody. *Am J Transplant*. 2012;12:313–321.
22. Akiyoshi T, Hirohashi T, Alessandrini A, et al. Role of complement and NK cells in antibody mediated rejection. *Hum Immunol*. 2012;73:1226–1232.
23. Hadad U, Martinez O, Krams SM. NK cells after transplantation: friend or foe. *Immunol Res*. 2014;58:259–267.
24. Zhang ZX, Huang X, Jiang J, et al. Natural killer cells mediate long-term kidney allograft injury. *Transplantation*. 2015;99:916–924.
25. Resch T, Fabritius C, Ebner S, et al. The role of natural killer cells in humoral rejection. *Transplantation*. 2015;99:1335–1340.
26. Kohei N, Tanaka T, Tanabe K, et al. Natural killer cells play a critical role in mediating inflammation and graft failure during antibody-mediated rejection of kidney allografts. *Kidney Int*. 2016;89:1293–1306.
27. Rajalingam R. The impact of HLA class I-specific killer cell immunoglobulin-like receptors on antibody-dependent natural killer cell-mediated cytotoxicity and organ allograft rejection. *Front Immunol*. 2016;7:585.
28. Venner JM, Hidalgo LG, Famulski KS, et al. The molecular landscape of antibody-mediated kidney transplant rejection: evidence for NK involvement through CD16a Fc receptors. *Am J Transplant*. 2015;15:1336–1348.
29. Gupta A, Broin PO, Bao Y, et al. Clinical and molecular significance of microvascular inflammation in transplant kidney biopsies. *Kidney Int*. 2016;89:217–225.
30. Dos Santos DC, Campos EF, Saraiva Camara NO, et al. Compartment-specific expression of natural killer cell markers in renal transplantation: immune profile in acute rejection. *Transpl Int*. 2016;29:443–452.
31. Legris T, Picard C, Todorova D, et al. Antibody-dependent NK cell activation is associated with late kidney allograft dysfunction and the complement-independent alloreactive potential of donor-specific antibodies. *Front Immunol*. 2016;7:288.
32. Parkes MD, Halloran PF, Hidalgo LG. Evidence for CD16a-mediated NK cell stimulation in antibody-mediated kidney transplant rejection. *Transplantation*. 2017;101:e102–e111.
33. Bachelet T, Couzi L, Lepreux S, et al. Kidney intragraft donor-specific antibodies as determinant of antibody-mediated lesions and poor graft outcome. *Am J Transplant*. 2013;13:2855–2864.
34. van Bergen J, Thompson A, Haasnoot GW, et al. KIR-ligand mismatches are associated with reduced long-term graft survival in HLA-compatible kidney transplantation. *Am J Transplant*. 2011;11:1959–1964.
35. Littera R, Piredda G, Argiolas D, et al. KIR and their HLA class I ligands: two more pieces towards completing the puzzle of chronic rejection and graft loss in kidney transplantation. *PLoS One*. 2017;12:e0180831.
36. Bjorkstrom NK, Ljunggren HG, Michaelsson J. Emerging insights into natural killer cells in human peripheral tissues. *Nat Rev Immunol*. 2016;16:310–320.
37. Muczynski KA, Leca N, Anderson AE, et al. Multicolor flow cytometry and cytokine analysis provides enhanced information on kidney transplant biopsies. *Kidney Int Rep*. 2018;3:956–969.
38. Loupy A, Haas M, Solez K, et al. The Banff 2015 Kidney Meeting Report: current challenges in rejection classification and prospects for adopting molecular pathology. *Am J Transplant*. 2017;17:28–41.
39. Haas M, Loupy A, Lefaucheur C, et al. The Banff 2017 Kidney Meeting Report: revised diagnostic criteria for chronic active T cell-mediated rejection, antibody-mediated rejection, and prospects for integrative endpoints for next-generation clinical trials. *Am J Transplant*. 2018;18:293–307.
40. Einecke G, Reeve J, Sis B, et al. A molecular classifier for predicting future graft loss in late kidney transplant biopsies. *J Clin Invest*. 2010;120:1862–1872.
41. Reeve J, Sellares J, Mengel M, et al. Molecular diagnosis of T cell-mediated rejection in human kidney transplant biopsies. *Am J Transplant*. 2013;13:645–655.
42. Schindelin J, Arganda-Carreras I, Frise E, et al. Fiji: an open-source platform for biological-image analysis. *Nat Methods*. 2012;9:676–682.
43. Rinaudo P, Boudah S, Junot C, et al. biosigner: a new method for the discovery of significant molecular signatures from omics data. *Front Mol Biosci*. 2016;3:26.
44. Abbas AR, Wolslegel K, Seshasayee D, et al. Deconvolution of blood microarray data identifies cellular activation patterns in systemic lupus erythematosus. *PLoS One*. 2009;4:e6098.